

Zeolitization of Tuffaceous Rocks in the Keşan Region, Thrace, Turkey

Fahri ESENLİ, Bektaş UZ, Fikret SUNER, Vildan ESENLİ, Ö. Işık ECE and Işık KUMBASAR

Key words: Analcime, Clinoptilolite, Heulandite, Mordenite, Tuffaceous rocks, Zeolitization, Thrace, Turkey.

Abstract

A 33 metre thick pyroclastic-rich zone of the Mezardere formation of Oligocene age is exposed in the Keşan region of Thrace, Turkey. In this zone, vitreous tuffs of dacitic composition have altered primarily to zeolites, including mordenite, heulandite–clinoptilolite and analcime. Silicification and alteration to clay minerals are common. Zeolite minerals have developed from volcanic glass, whereas some mordenites have formed from dissolution of heulandite-group zeolites. Although authigenic mineral paragenesis does not vary laterally, there is a marked vertical variation, particularly in zeolites. Mordenite (+heulandite–clinoptilolite) and analcime do not coexist and have formed in different stratigraphic levels. This suggests that their chemical environment is controlled by different hydrologic systems.

Whole rock composition shows the relationship between chemistry and secondary mineralogy. For example, whole rock trace element geochemistry indicates the natural selectivities of zeolites. There is also stratigraphic control on the chemistry and texture of mordenites. Specifically, $(Na+K)/(Ca+Mg)$ ratios of mordenites decrease from the lower to the upper levels. Mordenites of the lower level show a fibrous habit while the upper level mordenites are needle-like in shape. The average Si/Al ratio in mordenites is 3.90, in heulandite-group minerals 3.95, and in analcimes 2.34.

1. INTRODUCTION

The pyroclastic rocks have extensive zeolite reserves in nature. This is due to their high volcanic glass content and porosity. Composition of volcanic material as well as the ease of circulation of solutions influences dissolution of volcanic glass and the formation of zeolites. The crystallization sequence of minerals and reaction products during rock–solution interaction depends on the chemical composition of the starting material, contact of solution with volcanic glass and minerals of the pyroclastic rocks, rock–solution interaction time, temperature, pressure, pH, geological environment and hydrological systems (BOLES, 1988; BARTH-WIRSHING & HOLLER, 1989). Analcime, mordenite and clinoptilolite are usually regarded as diagenetic

products of glassy volcanic material. They can form in closed or open hydrological systems, in deep-sea sediments, in hydrothermal alteration zones and, as a result of low-grade burial metamorphism (IJIMA & UTADA, 1966; HAY, 1981; GOTTARDI & GALLI, 1985). The distribution of analcime-bearing and analcime-absent zones differs horizontally or vertically depending upon chemical zoning in these environments. Inner or deeper zones are characterized by the existence of analcimes (HAY, 1981).

Analcime is low silica zeolite, so that generally the Si/Al ratio is 2, while this ratio ranges from 2 to 3 for sedimentary analcimes (GOTTARDI & GALLI, 1985). Na is the only extra-framework cation in analcimes. Mordenite and heulandite–clinoptilolite are high silica zeolites. The Si/Al ratio of mordenites ranges from 4.2 to 5.9, and their cation contents per unit cell are 1.6–2.5 for Ca, 2.0–5.0 for Na and 0.1–0.8 for K (PASSAGLIA, 1975). However, in some examples K is reported as the dominant cation (COOMBS et al., 1997, and references therein). Heulandites have been distinguished from isostructural clinoptilolites on the basis of their Si/Al ratios – heulandites having $Si/Al < 4$ and clinoptilolites having $Si/Al > 4$. The clinoptilolite structure is more stable than that of heulandite and calcic clinoptilolite (MASON & SAND, 1960; ALIETTI, 1972; BOLES, 1972; ALIETTI et al., 1977). The cation contents in heulandites and clinoptilolites are highly variable and therefore Ca-, Na-, K- and Sr-heulandites and Ca-, Na- and K-clinoptilolites are commonly known (COOMBS et al., 1997).

The significance of zeolitization in tuffaceous rocks in SW Keşan (Thrace, northwest Turkey – Fig. 1), the occurrence, stratigraphic position and mineralogical characteristics of zeolite-bearing levels are discussed in this study. Some zeolite occurrences in the Upper Eocene–Oligocene pyroclastics from Thrace (in the vicinity of Gelibolu and Uzunköprü areas and the south-east of Keşan) have been previously reported (ESENLİ et al., 1997a; İÇÖZ & TÜRKMEÑOĞLU, 1997). These occurrences contain the heulandite–clinoptilolite type of zeolites in the Gelibolu and Uzunköprü areas and analcime and clinoptilolite in SE Keşan. In this study, the zeolites, including analcime, mordenite and heulandite–clinoptilolite, were described stratigraphically as alternate layers in the SW Keşan. The objective of this paper is to characterize the zeolitization and to explain the formation of analcime- and mordenite (+heulandite–clinoptilolite)-rich levels.

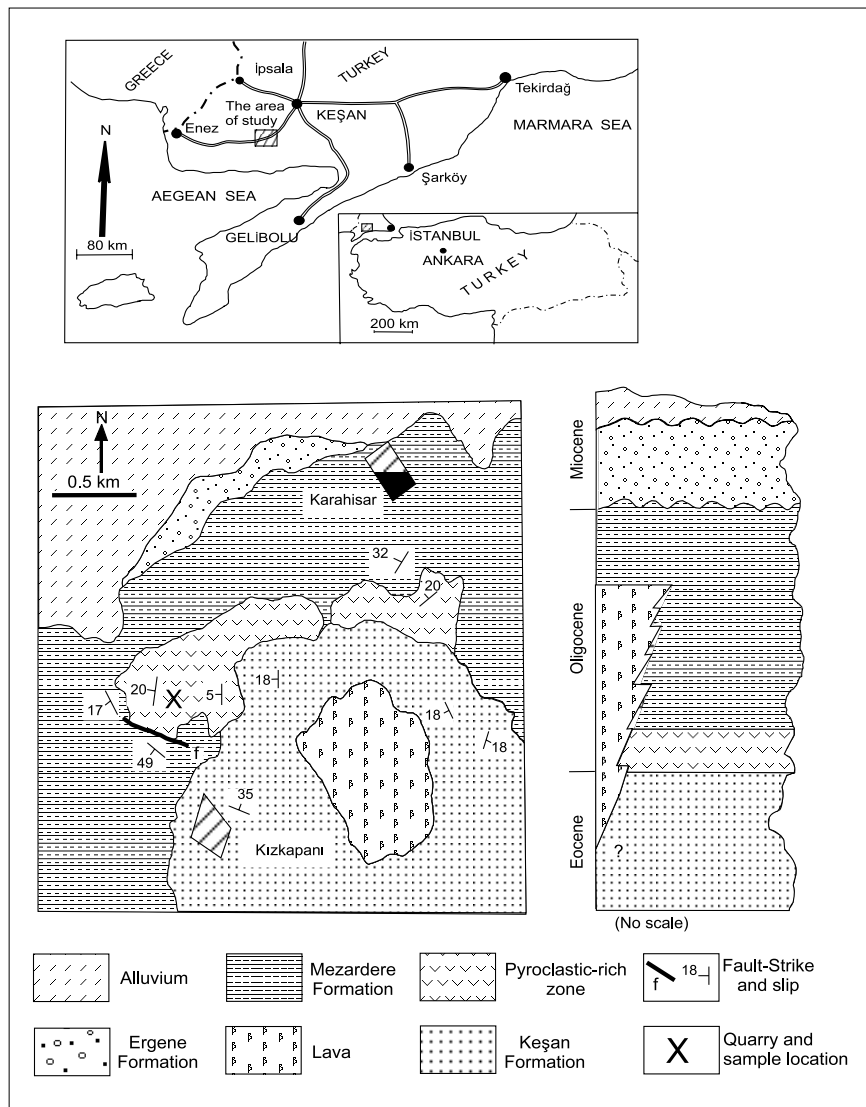


Fig. 1 The location, geological map and stratigraphic section of the study area (SW Keşan).

2. GEOLOGICAL SETTING

2.1. Thrace Basin

The Thrace basin is surrounded by the Stradja massif in the north, the Rhodope massif in the northwest and the Menderes metamorphic massif in the south. It is on the Intra-Pontide suture zone, which was developed by the northward subduction of the northern branch of the Neo Tethys Ocean during the Late Cretaceous–Early Tertiary period (ŞENGÖR & YILMAZ, 1981; YILMAZ et al., 1997) and continental collision of the Stradja and Sakarya zones (OKAY & TÜYSÜZ, 1999). The Thrace basin started to open at the end of the Middle Eocene, and sedimentation started as a transgressive process; however, environments of deposition significantly changed at the end of the Early Miocene and were later completed as regressive sedimentation (TURGUT et al., 1983, 1991). Thus, in the stratigraphic succession, fine-grained sediments of flysch facies proceed to shale, marl, limestone, coal and sandstone indicating lacustrine, fluvial and shallow marine depositional

environments. During the Late Oligocene–Early Miocene, the basin was wholly elevated and previously deposited sedimentary rocks were subjected to erosion. The Middle Miocene tectonic activity caused folding and faulting along the edges of the basin. During the Late Miocene, thick successions of conglomerate, sandstone, claystone and coal series were overlain on the pre-Miocene rocks across regional disconformities. The thickness of sedimentary rocks reaches up to 8 km in the centre of the Thrace basin (TURGUT et al., 1983, 1991).

Volcanic eruptions were synchronous with the maximum of the transgressive episode of the Thrace basin. Voluminous volcanic products with dacitic and andesitic composition form tuffaceous interbeds within sedimentary rocks or the tuffaceous matrix of clastic rocks. Petrographic and geochemical classification of the Thrace volcanic rocks presented by YILMAZ & POLAT (1998) and GENÇ (1998) are as follows: calc alkaline–intermediate volcanic products were extruded during the Late Eocene–Early Miocene period. This

first phase is assumed to be a product of Tibetan-type volcanism developed under the N–S compressional regime of northwestern Anatolia. The second volcanic phase started during the Late Miocene and is represented by alkaline basaltic lavas extruded sporadically in different parts of the Thrace region.

2.2. Keşan Region

The Keşan Formation (Upper Eocene) is the lowest part of the stratigraphic succession in the study area (SW Keşan, Fig. 1). It consists of turbiditic sandstones and minor shales and marls that are conformably overlain by the Lower–Middle Oligocene Mezardere Formation, described by TURGUT et al. (1983). The latter is unconformably overlain by the Miocene–Pliocene Ergene Formation. TURGUT et al. (1983) infers that the Keşan Formation was formed in a marine environment and the Mezardere Formation indicates lacustrine and shallow depositional environments. TERNEK (1949) and KOOP et al. (1969) described the volcanic activity (andesitic and dacitic lavas and tuffs) in the Keşan region throughout the Oligocene epoch. KOOP et al. (1969) reported an approximately 20 m thick pyroclastic bed named the “Keşan tuffs” between the Keşan and Mezardere Formations. Towards the Upper Oligocene, andesitic, dacitic and trachytic lavas became dominant. ERCAN et al. (1998) reported that andesitic lava from the Keşan area yields a K/Ar age of 26.2 ± 0.5 my (Late Oligocene, Chattian).

In the study area (SW Keşan, Fig. 1), tuffaceous rocks repeatedly occur both in the upper part of the Keşan Formation and throughout the Mezardere Formation. They are characterized by dacitic–andesitic tuffs interbedded with marls and sandstones. Zeolite-bearing tuffaceous rocks are constrained to the lower part of the Mezardere Formation, and are exposed between the villages of Karahisar and Kızkapanı in an area of about 1.5 km² (Fig. 1). The thickness of this zone is 33 m in a quarry in the Kızkapanı (see Fig. 5) and 20 m in the Karahisar areas. Trachytic lavas that appear as hills in the study area are probably younger than the pyroclastics.

3. METHODS

Nineteen samples have been studied stratigraphically in detail: fourteen zeolite-bearing pyroclastic, one non-zeolitic pyroclastic and four clastic rock samples. The samples were studied petrographically and mineralogically by polarizing microscope and X-ray diffractometer. A Philips diffractometer with Cu ($K\alpha$) radiation was used for X-ray powder diffraction (XRD) analyses and powder samples were scanned at $1^\circ 2\theta$ per minute. Major element compositions of rocks have been determined by the X-ray fluorescence (XRF) method. Powdered rock samples have been fused using LiBO₂ and the resulting glass disks have been analyzed in the

research laboratory of Turkish Glass Inc. Rigaku; Rix–2000 model equipment was used for XRF analyses. Trace elements were analyzed by using Spectro Ciros Vision ICP–ES for Ba and Sc (0.200 g pulp sample by LiBO₂ fusion) and Mo, Cu, Pb, Zn, Ni, As (0.50 g sample leached with 3 ml of 2–2–2 HCl–HNO₃–H₂O at 95°C for one hour, diluted to 10 ml) and by Perkin Elmer Elan 6100 ICP–MS for the other elements in the ACME Analytical Laboratories, Vancouver, Canada. Morphological characteristics and chemical compositions of zeolites (mordenite, analcime and heulandite–clinoptilolite) were investigated on a JSM–840 type scanning electron microscope (SEM) and a Tracor Northern 5400 energy dispersive X-ray spectrometer (EDX). Structural formulas of zeolite minerals were calculated on the basis of 72 oxygen for clinoptilolites and 96 oxygen for mordenites and analcimes using unnormalized oxide values. The quality of the analyses was calculated by evaluating the balance error given by GOTTARDI & GALLI (1985). The balance error of the mordenite and heulandite–clinoptilolite samples ranges 9–29% (however, Ba, Sr and Li were not analyzed).

4. RESULTS AND DISCUSSION

4.1. Whole Rock

The zeolite minerals are closely related to vitric tuffs of dacitic–andesitic composition. There is no clear difference in physical appearance between mordenite (+heulandite–clinoptilolite)-rich and non-zeolitic exposures in the field. They are massive and beige–pale green in colour. The analcime-rich outcrops, however, have a dark gray colour and are brittle which distinguishes them from the mordenite (+heulandite–clinoptilolite)-rich and non-zeolitic outcrops of tuffaceous rocks.

Phenocrysts of tuffs consist of plagioclase (oligoclase–andesine), biotite, amphibole (hornblende), quartz and opâque minerals. The phenocryst content ranges from 2 to 60 vol. %. Volcanic glassy material (glass shards and pumice fragments) has authigenetically transformed to zeolites (analcime, mordenite and heulandite–clinoptilolite), smectite (dioctahedral montmorillonite), silica minerals (opal-CT and quartz) and calcite. Mordenite, heulandite–clinoptilolite, smectite and opal-CT could not be identified optically. Analcimes are mostly anhedral. Calcites occur as pore-filling crystals as well as the alteration products of plagioclases. Quartz is present as both phenocrysts and as a secondary mineral, and the majority of it is of authigenic origin. The mineralogical compositions of the samples determined by XRD analysis are listed in Table 1. Samples from 1 to 19 are arranged stratigraphically from the lower to the upper zone (see Fig. 5). Samples numbered as 3, 7, 12 and 15 are of marl and sandy calcareous composition and the rest is of tuffaceous material. Sample 8 is the only pyroclastic rock which does not contain any

| Sample | Mineralogy |
|--------|--|
| 1 | Mordenite+Quartz |
| 2 | Mordenite+Quartz+Feldspar |
| 3 | Calcite+Quartz+Illite |
| 4 | Mordenite+Smectite+Quartz |
| 5 | Mordenite+Heulandite–Clinoptilolite+Smectite+Quartz |
| 6 | Mordenite+Heulandite–Clinoptilolite+Smectite |
| 7 | Calcite+Quartz+Illite+Kaolinite+Feldspar |
| 8 | Quartz+Feldspar+Calcite+Illite |
| 9 | Analcime+Quartz+Feldspar |
| 10 | Quartz+Mordenite+Heulandite–Clinoptilolite+Opal-CT+Feldspar+Smectite |
| 11 | Mordenite+Quartz+Heulandite–Clinoptilolite+Opal-CT+Calcite |
| 12 | Quartz+Calcite+Feldspar |
| 13 | Mordenite+Smectite+Opal-CT+Feldspar+Calcite+Quartz |
| 14 | Analcime+Quartz+Smectite+Feldspar |
| 15 | Quartz+Calcite+Kaolinite+Illite+Feldspar |
| 16 | Smectite+Mordenite+Feldspar |
| 17 | Mordenite+Quartz+Feldspar+Smectite |
| 18 | Mordenite+Quartz+Smectite |
| 19 | Mordenite+Quartz+Feldspar+Heulandite–Clinoptilolite+Smectite |

Table 1 The mineralogical composition of pyroclastic and clastic rocks of SW Keşan determined by XRD.

zeolite mineral. Mordenite is identified in twelve samples and analcime is found only in samples 9 and 14. These minerals are generally the major components of rock samples according to the XRD patterns (Fig. 2). Analcime- and mordenite-bearing levels alternate in the stratigraphic sequence. Lesser amounts of heulandite–clinoptilolite are associated with mordenite in five samples (5, 6, 10, 11 and 19). Smectite is identified in ten samples, and it is the main mineral in sample 16. Opal-CT in three samples is from the middle level of the zeolite-bearing zone.

The major element compositions of nine rock samples and trace element analyses of eleven samples are given in Tables 2 and 3, respectively. Plotted on the

Zr/TiO₂–Nb/Y diagram of WINCHESTER & FLOYD (1977), most of the samples fall in the dacite–rhyodacite field (Fig. 3). Only sample 5 is trachyandesite and sample 9 is andesite. There is a relationship between the whole rock chemistry and secondary mineralogy of the samples. For example, the SiO₂ content of analcime-rich samples is low, but high in mordenite-rich samples. CaO, except sample 8, is between 3.23 and 4.17 wt. %. The high CaO of sample 8 (9.17%) is probably due to the presence of calcite in this sample. Fe₂O₃ contents of samples 8, 9, 11, 14 and 16 are higher than those of other samples. According to the XRD results, sample 8 contains a trace amount of illite. On the other hand, thin-section observations revealed that illite–celadonite minerals seen in the matrix, in voids and in pheno-

| | Sample | | | | | | | | |
|--------------------------------|--------|-------|-------|-------|-------|-------|-------|-------|-------|
| | 1 | 5 | 8 | 9 | 11 | 14 | 16 | 18 | 19 |
| SiO ₂ | 65.91 | 66.17 | 56.60 | 61.07 | 65.49 | 61.47 | 63.22 | 66.43 | 67.36 |
| Al ₂ O ₃ | 14.01 | 13.49 | 14.00 | 16.01 | 13.50 | 15.45 | 14.18 | 13.29 | 13.93 |
| Fe ₂ O ₃ | 1.61 | 1.31 | 5.57 | 2.74 | 3.47 | 2.84 | 3.01 | 1.82 | 1.76 |
| MnO | 0.16 | 0.21 | 0.28 | 0.11 | 0.05 | 0.16 | 0.17 | 0.17 | 0.10 |
| TiO ₂ | 0.28 | 0.34 | 0.85 | 0.64 | 0.35 | 0.42 | 0.60 | 0.38 | 0.33 |
| MgO | 1.31 | 1.71 | 2.35 | 2.37 | 1.63 | 2.20 | 2.85 | 1.90 | 1.98 |
| CaO | 3.51 | 3.54 | 9.17 | 3.53 | 3.30 | 3.28 | 3.12 | 4.17 | 3.23 |
| K ₂ O | 1.66 | 2.65 | 2.98 | 1.95 | 2.92 | 2.10 | 2.83 | 2.87 | 2.74 |
| Na ₂ O | 2.88 | 1.50 | 2.59 | 3.90 | 0.71 | 4.15 | 1.31 | 1.33 | 1.18 |
| P ₂ O ₅ | 0.11 | 0.07 | 0.35 | 0.14 | 0.08 | 0.13 | 0.13 | 0.12 | 0.09 |
| LOI | 8.56 | 8.01 | 5.26 | 7.54 | 8.50 | 7.80 | 8.58 | 7.52 | 7.30 |

Table 2 Whole rock chemistry (wt. %) of the samples.

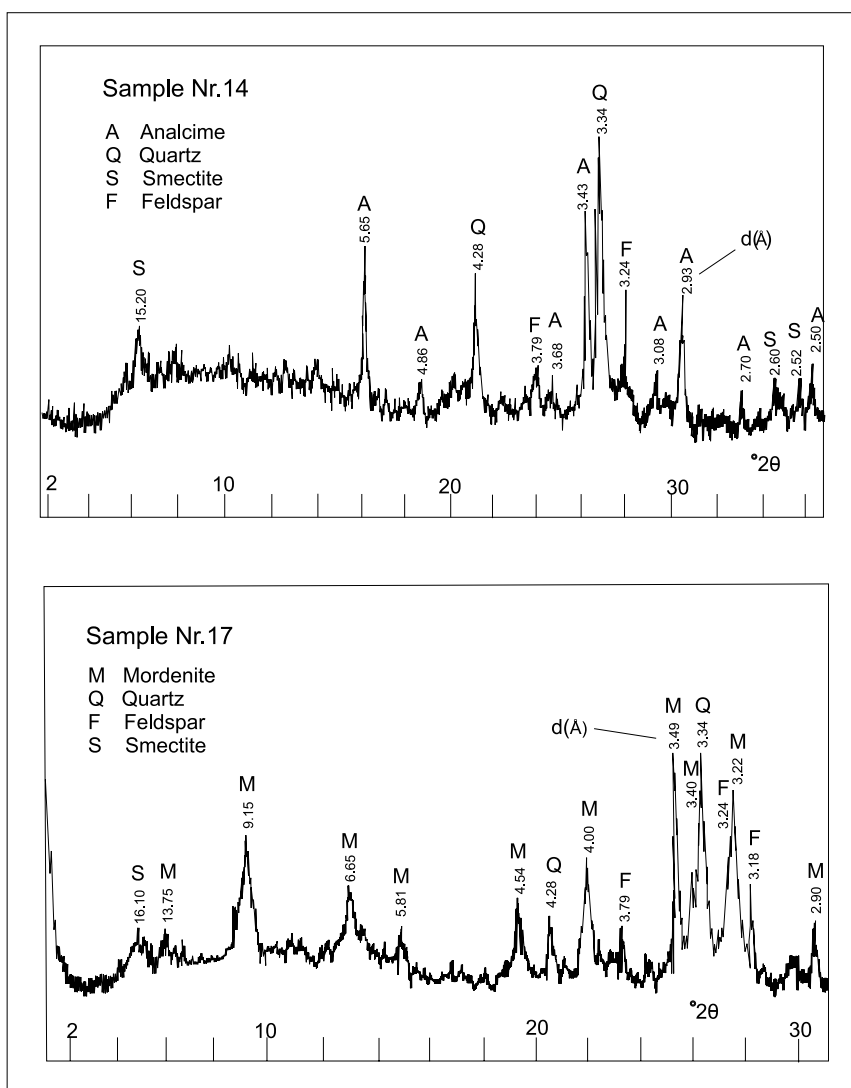


Fig. 2 The XRD patterns of analcime- and mordenite-bearing samples (a: sample 14, and b: sample 17).

crystals of samples 8, 9, 10, 11 and 14, are products of alteration. These clay-group minerals were not detected in XRD patterns except in sample 8. Therefore the presence of illite–celadonite minerals might explain the high Fe_2O_3 in samples 8, 9, 11, 14 and 16. In addition, mordenites in these samples also contribute some amounts of iron. Indeed, single crystal analyses (Table 4) show that mordenites have a high content of Fe. K_2O and Na_2O range between 1.66–2.98% and 0.71–4.15%, respectively. Na_2O of the non-zeolitic sample 8 is higher than that of mordenite-rich samples and reaches its highest values in analcime-rich samples. The results of the trace element chemistry can be summarized as follows: (a) Co, V, Zn, Ni, Y, Sm, Eu, Gd, Tb, Dy, Tb, Ho, Er are higher in sample 8 containing no authigenic zeolite mineral; (b) Samples 9 and 14 are richer in analcime and Cs, Mo, Rb, U, Zr, Cu, Pb are higher in these samples, and (c) Ba, Sr, Th, La, Ce and As of mordenite-bearing samples 1, 5, 10, 11, 13, 16, 18 and 19 (Table 3), are higher than the average values of all other samples studied. It is also determined that samples containing mordenite+heulandite–clinoptilolite have higher average values for Ba and Sr than those of the morde-

nite-rich group. On the other hand, considering the stratigraphic positions of mordenite-bearing samples, the upper levels are richer in Ba, Rb, Sr, Ti, U, W and As, while the lower levels are richer in Mo, Cu, Pb, Zn, and Y–Lu series.

4.2. Zeolites

Mordenites of the tuffaceous rocks (SW Keşan) show fibrous and needle-like habits (Figs. 4a and b). The mordenite needles are about 3–20 μm in length and 0.3–1 μm in width, whereas the widths of fibres of thread-like mordenites are generally less than 0.2 μm . Mordenites have formed as individual crystal and also as radial from a nucleus (Fig. 4c). They have mostly developed from volcanic glassy material. The fibres are growing from the top of the vitrified volcanic glass, which displays a parallel fractured alteration pattern as shown in Fig. 4d. However, some mordenites of sample 19 have been observed as tiny crystals on heulandite-group crystals (Fig. 4e). In this case, heulandites–clinoptilolites transformed to mordenite crystals which were in the form of dissolved grains and do not exhibit their

| | Sample | | | | | | | | | | |
|----|--------|------|------|------|------|------|------|-------|------|------|------|
| | 1 | 5 | 8 | 9 | 10 | 11 | 13 | 14 | 16 | 17 | 18 |
| As | 4 | 17 | 3 | 4 | 4 | 5 | 4 | 3 | 4 | 5 | 4 |
| Ba | 658 | 1585 | 333 | 623 | 1020 | 873 | 698 | 210 | 636 | 571 | 869 |
| Ce | 57.9 | 55.4 | 50.7 | 56.8 | 52.1 | 64.0 | 62.0 | 55.1 | 59.8 | 63.5 | 58.3 |
| Co | 6.3 | 1.8 | 12.6 | 7.7 | 5.3 | 3.6 | 3.9 | 4.0 | 6.9 | 6.8 | 7.7 |
| Cs | 4.3 | 2.9 | 2.9 | 11.3 | 2.5 | 2.6 | 3.1 | 12.2 | 4.4 | 3.0 | 5.3 |
| Cu | 9 | 4 | 6 | 11 | 10 | 6 | 6 | 7 | 7 | 6 | 8 |
| Dy | 2.33 | 1.46 | 3.72 | 2.94 | 2.73 | 2.47 | 2.56 | 2.50 | 2.47 | 2.25 | 2.29 |
| Er | 1.49 | 1.11 | 2.23 | 1.85 | 1.45 | 1.70 | 1.69 | 1.67 | 1.65 | 1.22 | 1.55 |
| Eu | 0.62 | 0.44 | 1.25 | 0.89 | 0.67 | 0.68 | 0.76 | 0.71 | 0.7 | 0.67 | 0.59 |
| Ga | 14.7 | 13.4 | 15.0 | 15.3 | 11.9 | 14.5 | 15.4 | 13.9 | 15.8 | 13.7 | 14.7 |
| Gd | 2.58 | 1.93 | 4.37 | 3.57 | 2.42 | 2.61 | 2.64 | 3.15 | 2.82 | 2.33 | 2.74 |
| Hf | 4.3 | 4.2 | 4.6 | 5.1 | 3.6 | 4.7 | 5.0 | 5.0 | 4.7 | 4.1 | 4.3 |
| Ho | 0.43 | 1.31 | 0.78 | 0.62 | 0.48 | 0.51 | 0.52 | 0.50 | 0.51 | 0.41 | 0.48 |
| La | 32.1 | 35.6 | 24.6 | 31.6 | 30.0 | 36.0 | 35.3 | 30.0 | 33.2 | 34.1 | 30.1 |
| Lu | 0.22 | 0.21 | 0.34 | 0.35 | 0.27 | 0.32 | 0.34 | 0.30 | 0.29 | 0.28 | 0.26 |
| Nb | 7.6 | 8.2 | 6.2 | 8.7 | 7.0 | 9.1 | 8.6 | 10.5 | 9.1 | 7.6 | 7.7 |
| Nd | 18.9 | 17.1 | 24.2 | 21.1 | 18.4 | 22.4 | 21.4 | 21.2 | 22.7 | 20.6 | 20.1 |
| Ni | 7 | 4 | 18 | 13 | 6 | 2 | 3 | 17 | 13 | 7 | 14 |
| Mo | 0.3 | 0.4 | 0.3 | 1.1 | 0.6 | 0.2 | 0.3 | 0.2 | 0.2 | 0.4 | 0.2 |
| Pb | 33 | 39 | 1 | 32 | 28 | 35 | 35 | 23 | 39 | 36 | 33 |
| Pr | 5.83 | 5.60 | 6.16 | 6.20 | 5.49 | 6.61 | 6.4 | 5.76 | 6.32 | 6.09 | 5.60 |
| Rb | 89.8 | 77.5 | 69.2 | 91.0 | 85.5 | 65.4 | 72.8 | 100.7 | 75.0 | 78.0 | 77.3 |
| Sm | 3.4 | 2.6 | 5.2 | 4.0 | 3.0 | 3.8 | 3.6 | 3.3 | 3.9 | 3.2 | 3.5 |
| Sr | 1112 | 1882 | 433 | 731 | 1679 | 1585 | 1060 | 201 | 819 | 920 | 1232 |
| Ta | 0.7 | 0.7 | 0.3 | 0.6 | 0.6 | 0.7 | 0.6 | 0.7 | 0.7 | 0.7 | 0.7 |
| Tb | 0.42 | 0.30 | 0.73 | 0.57 | 0.42 | 0.44 | 0.5 | 0.43 | 0.48 | 0.38 | 0.43 |
| Th | 18.7 | 1.8 | 6.9 | 17.7 | 16.3 | 23.6 | 19.8 | 16.6 | 19.7 | 17.7 | 18.0 |
| Tl | 0.8 | 0.5 | 0.5 | 0.6 | 0.3 | 0.4 | 0.3 | 0.3 | 0.2 | 0.5 | 0.5 |
| Tm | 0.25 | 0.17 | 0.31 | 0.32 | 0.25 | 0.29 | 0.32 | 0.25 | 0.27 | 0.21 | 0.27 |
| U | 4.4 | 13.3 | 2.1 | 6.7 | 5.5 | 7.1 | 7.2 | 5.5 | 5.3 | 4.4 | 6.2 |
| V | 42 | 35 | 113 | 62 | 50 | 29 | 43 | 42 | 48 | 33 | 53 |
| W | 3 | 4 | 1 | 2 | 1 | 1 | 1 | 1 | 1 | 3 | 2 |
| Y | 14.6 | 9.8 | 21.7 | 20.1 | 14.8 | 17.2 | 17.9 | 17.2 | 16.5 | 13.0 | 15.1 |
| Yb | 1.91 | 1.23 | 2.24 | 2.06 | 1.62 | 2.02 | 2.21 | 1.88 | 1.76 | 1.53 | 1.70 |
| Zn | 36 | 23 | 50 | 47 | 35 | 30 | 29 | 37 | 43 | 31 | 36 |
| Zr | 141 | 157 | 156 | 162 | 128 | 153 | 172 | 167 | 178 | 143 | 138 |

Table 3 Whole rock trace element composition (ppm) of the samples.

monoclinic idiomorphic habits. These heulandite-group minerals were probably transformed to mordenites after dissolution. PE-PIPER (2000) reported transformations between heulandite-group and mordenite-group minerals, which are depending on the changes in temperature. KITSOPULOS (1997) also reported the mordenites from the Polyegos Island, Greece, which are draped over and formed from the crystals of heulandites.

The average structural formulae of the Keşan mordenites was calculated on the basis of 96 oxygen to $[\text{Ca}_{1.7}\text{Mg}_{1.3}\text{Na}_{2.0}\text{K}_{1.6}] [(\text{Fe}, \text{Al})_{9.6}\text{Si}_{37.4}\text{O}_{96}] \cdot 28\text{H}_2\text{O}$. They show the Si/Al ratio ranging from 3.60 to 4.36 with an average value of 3.9 and the average value of

the (Na+K)/(Ca+Mg) ratio is 1.2 ranging from 0.90 to 1.57 (Table 4). The obtained Si/Al ratio is lower than those corresponding to hydrothermal mordenites. PAS-SAGLIA (1975) showed that there are no large variations in the chemical composition of mordenites with probably sedimentary and hydrothermal origin, however, according to GODOVIKOV (1985) hydrothermal mordenites have higher silica and water contents than sedimentary mordenites. Chemical compositions of the Keşan mordenites exhibit variations across the stratigraphic sequence (see Table 4 and Fig. 5). The ratio of alkali/earth alkali cations decreases toward the upper levels. This difference can be clearly seen in the com-

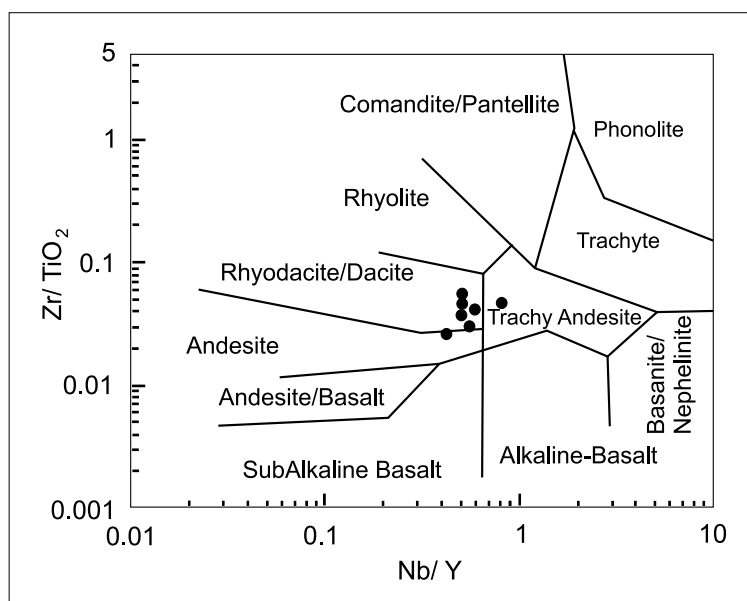


Fig. 3 Classification of samples based on Zr/TiO_2 vs. Nb/Y diagram of WINCHESTER & FLOYD (1977).

parison of mordenites from the lower and upper levels. Cation contents change from $[Ca_{1.0} Mg_{1.5} Na_{1.2} K_{2.7}]$ for the lower level mordenites (sample 1) to $[Ca_{2.0} Mg_{2.1} Na_{3.3} K_{0.5}]$ for the upper level mordenites (sample 19). Mordenites of the lower level are poor in Na and Ca and rich in K, whereas mordenites of the upper levels are poor in K and rich in Na and Ca. Morphological properties of these mordenites from the lower level, even the middle levels (samples 6 and 11), show a fibrous habit and mordenites from the upper level are needle-like in shape (Figs. 4a and b). Consequently, fibrous mordenites are rich in K and needle-like mordenites are rich in Ca and Na in the Keşan region. STOCIA et al. (1992) showed that structural changes of mordenite-group minerals are due to chemical and thermal differentiation. HAWKINS (1981) also concluded that mordenites had a more tabular than fibrous morphology when they tended to be rich in Ca. Likewise, Ca-rich mordenites in the Şile region (NW İstanbul, Turkey) displayed pris-

matic crystals with c-elongation similar to those of epistilbites (ESENLI et al., 1997b). In spite of the fact that typically tabular mordenite have not been found in the Keşan samples, the relationship between the chemistry and morphology of fibrous and needle-like mordenites from the SW Keşan supports these findings. Furthermore, RUDOLF & GARCES (1994) reported the relationships between Si/Al ratios, c-dimensions and X-ray patterns of mordenites. But, the X-ray patterns and Si/Al ratios of the Keşan mordenites collected from different stratigraphic levels do not show any significant difference. XRD patterns of mordenite are slightly broadened (Fig. 2b). The d-spacing values (Å) of principal reflections of all studied mordenites are 3.49, 3.22, 9.15, 4.00, 3.40, 6.65 and 4.54.

Heulandite-group minerals were found to have developed directly from volcanic glass. Although, the existence of heulandite-clinoptilolite minerals in the Keşan

| Sample (Mineral) | 1 (M) | 6 (M) | 6 (M) | 6 (H-C) | 9 (A) | 11 (M) | 11 (H-C) | 14 (A) | 19 (M) | 19 (H-C) |
|------------------|-------|-------|-------|---------|-------|--------|----------|--------|--------|----------|
| Si | 37.45 | 37.68 | 37.64 | 28.07 | 33.87 | 36.83 | 29.80 | 34.92 | 37.38 | 27.87 |
| Al | 9.57 | 9.93 | 9.60 | 7.65 | 14.94 | 10.24 | 6.32 | 14.50 | 8.57 | 8.07 |
| Fe | 1.25 | 0.74 | 1.19 | 0.37 | 0.06 | 0.61 | 0.23 | 0.32 | 1.31 | 0.14 |
| Ti | 0.22 | 0.16 | 0.09 | 0.09 | – | 0.09 | – | – | 0.22 | 0.14 |
| Mg | 1.50 | 0.90 | 0.82 | 0.90 | 0.38 | 1.19 | 0.77 | – | 2.13 | 1.22 |
| Ca | 0.97 | 1.74 | 1.85 | 2.13 | 0.22 | 1.83 | 1.09 | 0.16 | 2.03 | 1.91 |
| K | 2.69 | 1.37 | 2.32 | 0.60 | 0.06 | 0.98 | 0.50 | 0.06 | 0.50 | 0.37 |
| Na | 1.19 | 1.99 | 1.25 | 0.70 | 10.27 | 2.13 | 0.86 | 10.34 | 3.25 | 0.69 |
| Si/Al | 3.91 | 3.79 | 3.92 | 3.67 | 2.27 | 3.60 | 4.72 | 2.41 | 4.36 | 3.45 |
| Na+K/Mg+Ca | 1.57 | 1.27 | 1.34 | 0.42 | – | 1.03 | 0.73 | – | 0.90 | 0.34 |
| Error % | 22.6 | 23.4 | 21.1 | 8.9 | 30.1 | 18.5 | 28.9 | 38.2 | 18.1 | 12.1 |

Table 4 The unit-cell compositions of heulandite-clinoptilolite (H-C), mordenite (M) and analcime (A).



Fig. 4 Photomicrographs of zeolite minerals: (a) fibrous mordenites in the sample 1; (b) needle-like mordenites in the sample 19; (c) needle-like mordenites with radial habit in sample 19; (d) fibrous mordenites which are growing from volcanic glass in the sample 1; (e) mordenites over the anhedronal heulandite-group minerals in sample 6; (f) analcime in volcanic glassy material in sample 14.

samples were determined by XRD studies, their typical crystal habit (monoclinic plate) was not observed in SEM studies. These grains are generally anhedronal in shape and about 5 μm long (Fig. 4e). The average structural formulae of the Keşan heulandite-group zeolites was calculated on the basis of 72 oxygen to $[\text{Ca}_{1.7} \text{Mg}_{1.0} \text{Na}_{0.8} \text{K}_{0.5}] [\text{Al}_{7.4} \text{Si}_{28.6} \text{O}_{72}] \cdot 24\text{H}_2\text{O}$. This formula is close to the clinoptilolite-Ca referred by COOMBS et al. (1997). Si/Al ratios of the Keşan heulandite-group zeolites range from 3.45 to 4.72 and their average value is 3.95 (Table 4). According to this ratio, some of the

analyzed heulandite-group zeolites are clinoptilolite while the others can be classified as heulandite. Their $(\text{Na}+\text{K})/(\text{Ca}+\text{Mg})$ ratios have an average value of 0.50 and range from 0.34 to 0.73.

Analcimes were observed by both optical microscopy and SEM as idiomorphous and hypidiomorphous crystals, mainly bedded in volcanic glass (Fig. 4f). These minerals were generally below 0.05 mm in size. No transformation from any phenocrysts and zeolite mineral to analcime was observed; it occurred directly from volcanic glassy materials. The XRD patterns of

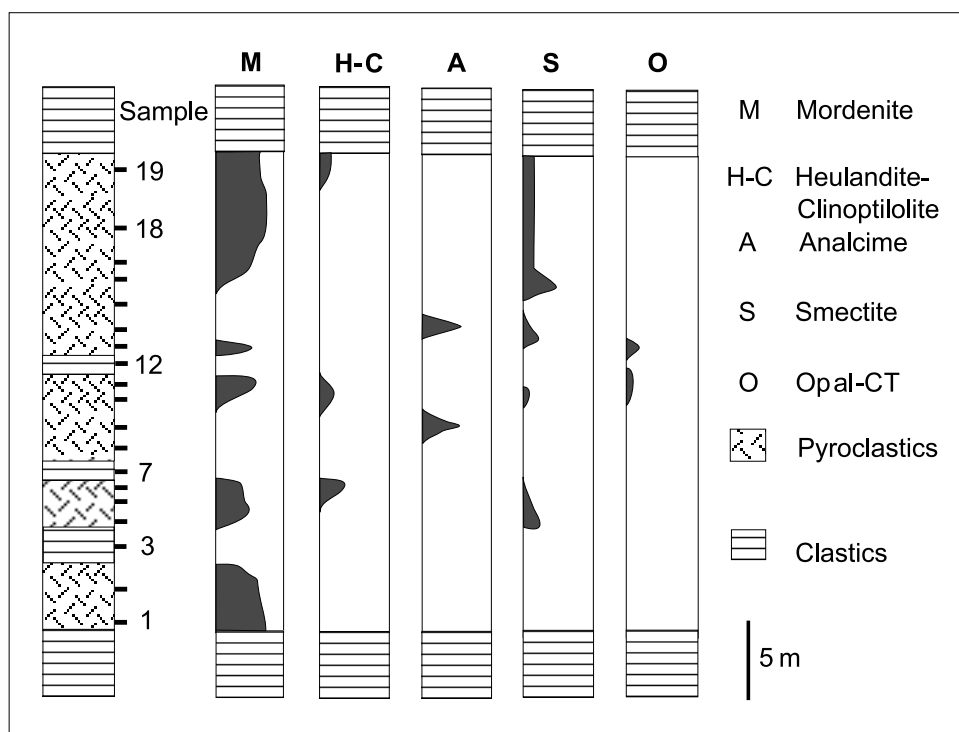


Fig. 5 Stratigraphically, relative abundances of authigenic minerals in the study area (SW Keşan).

analcime are very sharp (Fig. 2a) and spacing values (\AA) of the most important lines are 3.43, 5.65, 2.93 and 2.50 in order of their relative intensities. The chemistry of analcime (Table 4) was slightly consistent with the typical unit-cell formula reported in the literature (MUMPTON, 1981; GOTTARDI & GALLI, 1985). The Keşan analcimes had a high content of Si and lesser content of Al and Na. The average value of the Si/Al ratio of two analcime grains was 2.34.

4.3. Occurrence

The relative abundance and stratigraphic distributions of authigenic minerals of the pyroclastic-rich zone of the Mezardere formation are shown in Fig. 5. Mordenite and heulandite-clinoptilolite are the most and the least abundant zeolite minerals in this zone, respectively (Table 1 and Fig. 5). These two minerals exist together at a level where analcime is absent. There are two separate analcime-rich levels in the middle parts of the zone (Fig. 5). Smectite is associated with all zeolite minerals and its abundance increases upward. Opal-CT is observed in minor amounts in association with mordenite and heulandite-group zeolites in the middle levels. No petrographic evidence is found to suggest the time relationships for the occurrences of opal, smectite and zeolites. Authigenic quartz commonly occurs with analcimes.

Zeolitic tuffaceous rocks in the Keşan region are interbedded with Lower Oligocene sediments of lacustrine and shallow marine environments. Zeolitization is limited only to pyroclastics and not found in epiclastics. The recurrent alternate horizons of mordenite

(+heulandite-clinoptilolite) and analcime in about a 30 m thick zone could not be explained by variation of marine water chemistry. It is difficult to explain how major changes of shallow marine water composition can take place within short time intervals. Therefore, the zeolitization in the Keşan seems not to be developed in a marine environment. Moreover, the formation of analcime and mordenite in different levels could not be related to the chemistry of the host rock. Chemical composition and petrographic characteristics of rocks where the zeolitization took place show no distinct variation with stratigraphy.

Zeolitization probably took place in a lacustrine environment, being exposed to an open hydrological system. No lateral zonation of authigenic minerals was observed throughout the area (between the Kızıkapını and Karahisar localities). This implies that zeolitization took place at constant conditions laterally. But, as seen in Fig. 5, vertical mineralogical zonation was clearly observed in the field. The vertical variation of petrographic and mineralogical composition of the tuffaceous rocks (Fig. 5) can be examined in a quarry in the Kızıkapını area. But, the exposures of tuffaceous rocks are limited in the Karahisar area. In this area, mordenite-rich levels correspond stratigraphically to the mordenite-rich upper levels of the Kızıkapını section (Fig. 5). However, the lower levels of the Karahisar section have not been observed in the field, and thus no information was available. Taking only the upper levels of pyroclastics in two areas into consideration, there is no evidence showing the lateral variation in zeolitization.

During zeolitization, the fluid chemistry probably changed over short time intervals. Hydrological and

mineralogical boundaries have also changed as they were controlled by climatic parameters. Conditions in open hydrological systems have probably changed to those of a closed lacustrine environment causing alkali enrichment in the water. Two analcime-rich levels must have developed due to these changes. Such environmental changes took place during the Oligocene–Miocene in the Thrace region, especially in the south Thrace (TURGUT et al., 1983).

In Oligocene time, the chemistry of pore water and ground water was suitable for the development of mordenites (stratigraphically lower level in Fig. 5) in the Keşan region (actually SW Keşan). Towards the end of this period, first smectite and then heulandite–clinoptilolite became associated with mordenite. Later, the following products formed sequentially: (a) analcime, (b) mordenite (mordenite+heulandite–clinoptilolite+smectite+opal-CT), (c) second analcime, and finally (d) a longer mordenite formation period. Still later, smectite and heulandite–clinoptilolite association formed with mordenite. Zeolitization in the Keşan region have been controlled by the variation of water chemistry through time.

5. CONCLUSIONS

In SE Keşan the stratigraphically lower zone of the tuffaceous rocks of Oligocene age have undergone zeolitic alteration. This process has created a vertical zone of different zeolite minerals. Parent material, mainly volcanic glass, has been transformed to zeolite minerals by the action of fluids probably in an open hydrological regime. However, there must be several intervals affected by various parameters during this episode. Thus, analcime- and mordenite(+heulandite–clinoptilolite)-rich levels formed repeatedly in the study area. The stratigraphic sequence of zeolite mineral paragenesis of at 30 metre thick tuffaceous zone can be summarized as: (mordenite) → (mordenite+heulandite–clinoptilolite) → (analcime) → (mordenite+heulandite–clinoptilolite) → (mordenite) → (analcime) → (mordenite) → (mordenite+heulandite–clinoptilolite). This mineralogical sequence reflects the changes in hydrological systems and chemistry of waters during the zeolitization processes and emphasized the variation in geological environments. In the Early Oligocene changes in the climate and depth of the lake water must have taken place in the SW Thrace. The mineralogical data presented in this paper agree with previously reported geological observations in Thrace by TURGUT et al. (1983, 1991).

Acknowledgements

The authors thank Dr. Attila KILINÇ who read and improved the text. Comments and review by Professor Darko TIBLJAŠ and Professor Vladimir BERMANEC are gratefully acknowledged.

6. REFERENCES

- ALIETTI, A. (1972): Polymorphism and crystal-chemistry of heulandites and clinoptilolites.– *American Mineralogist*, 57, 1448–1462.
- ALIETTI, A., BRIGATTI, M.F. & POPPI, L. (1977): Natural Ca-rich clinoptilolites (heulandite of group 3): New data review.– *Neues Jahrbuch für Mineralogie–Monatshefte*, H11, 493–501.
- BARTH-WIRSHING, U. & HOLLER, H. (1989): Experimental studies on zeolite formation conditions.– *European Journal of Mineralogy*, 1, 489–506.
- BOLES, J.R. (1972): Composition, optical properties, cell dimensions and thermal stability of some heulandite-group zeolites.– *American Mineralogist*, 57, 1463–1493.
- BOLES, J.R. (1988): Occurrences of natural zeolites. Present status and future research.– In: KALLO, D. & SHARRY, H.S. (eds.): *Occurrence, Properties and Utilization of Natural Zeolites*. Akademiai Kiado, Budapest, 3–18.
- COOMBS, D.S., ALBERTI, A., ARMBRUSTER, T., ARTIOLI, G., COLELA, C., GALLI, E., GRICE, J.D., LIEBAU, F., MANDARINO, J.A., MINATO, H., NICKEL, E.H., PASSAGLIA, E., PEACOR, D.R., QUARTIERI, S., RINALDI, R., ROSS, M., SHEPPARD, R.A., TILLMANS, E. & VEZZALINI, G. (1997): Recommended nomenclature for zeolite minerals: Report of the Subcommittee on zeolites of the International Mineralogical Association, Commission on New Minerals and Mineral Names.– *The Canadian Mineralogist*, 35, 1571–1606.
- ERCAN, T., TÜRKECAN, A., GÜLLOU, H., SATIR, M., SEVİN, D. & ŞAROĞLU, F. (1998): Marmara Denizi çevresindeki Tersiyer volkanizmasının özellikleri [*Tertiary volcanism around the sea of Marmara – in Turkish*].– *MTA Bulletin*, 120, 199–221.
- ESENLİ, F., UZ, B., EREN R.H., COBAN, F., MANAV, H., YAVUZ, O. & KUMBASAR, I. (1997a): Alteration products of pyroclastic rocks in Thrace, Turkey.– In: PAPUNEN, H. (ed.): *Proceeding of the 4. Biennial SGA Meeting – Mineral Deposits, Turku*, 713–716.
- ESENLİ, F., UZ, B. & KUMBASAR, I. (1997b): Mordenite type zeolite occurrence in the Upper Cretaceous volcanics of Şile region, İstanbul–Turkey.– *Geological Bulletin of Turkey*, 40, 43–49.
- GENÇ, Ş.C. (1998): Evolution of the Bayramiç magmatic complex, northwestern Anatolia.– *Journal of Volcanology and Geothermal Research*, 85, 233–249.
- GODOVIKOV, A. (1985): *Mineralogy*.– Mir, Moscow, 582 p.
- GOTTARDI, G. & GALLI, E. (1985): *Natural Zeolites*.– Springer Verlag, Berlin, 409 p.
- HAWKINS, D.B. (1981): Kinetics of glass dissolution and zeolite formation under hydrothermal conditions.– *Clays and Clay Minerals*, 29, 331–340.
- HAY, R.L. (1981): Geology of zeolites in sedimentary rocks.– In: MUMPTON, F.A. (ed.): *Mineralogy and Geology of Natural Zeolites. Reviews in Mineralogy, Mineralogical Society of America*, Washington D.C., 53–64.
- İÇÖZ, S. & TÜRKMEÑOĞLU, A. (1997): Eosen-Oligosen yaşlı klastiklerin (Keşan, Trakya) mineralojik, petrografik ve jeokimyasal incelenmesi [*The mineralogic,*

- petrographic and geochemical investigation of Eocene–Oligocene clastics, Keşan, Thrace – in Turkish].– In: IŞIK, İ. (eds.): Proceeding of the National Clay Symposium. Kütahya, 37–48.*
- IJIMA, A. & UTADA, M. (1966): Zeolites in sedimentary rocks with reference to the depositional environments and zonal distribution.– *Sedimentology*, 7, 327–357.
- KITSOPULOS, K.P. (1997): The genesis of a mordenite deposit by hydrothermal alteration of pyroclastics on Polyegos island, Greece.– *Clays and Clay Minerals*, 45, 632–648.
- KOOP, K.O., PAVONI, N. & SCHINDLER, C. (1969): Geologie Thrakiens. Das Ergene Becken.– *Beihefte zum Geologischen Jahrbuch*, 76, 171 p.
- MASON, B. & SAND, L.B. (1960): Clinoptilolite from Patagonia. The relationship between clinoptilolite and heulandite.– *American Mineralogist*, 45, 341–350.
- MUMPTON, F. (1981): Natural zeolites.– In: MUMPTON, F.A. (ed.): *Mineralogy and Geology of Natural Zeolites. Reviews in Mineralogy*, Mineralogical Society of America, Washington D.C., 1–15.
- OKAY, A.I. & TÜYSÜZ, O. (1999): Tethyan sutures of northern Turkey.– In: DURAND, B., JOLIVET, L., HORVATH, F. & SERANNE, M. (eds.): *The Mediterranean Basins: Tertiary Extension within the Alpine Orogen*. Geological Society of London, Spec. Publ., 156, 475–515.
- PASSAGLIA, E. (1975): The crystal chemistry of mordenites.– *Contributions to Mineralogy and Petrology*, 50, 65–77.
- PE-PIPER, G. (2000): Mode of occurrence, chemical variation and genesis of mordenite and associated zeolites from the Mordem area, Nova Scotia, Canada.– *The Canadian Mineralogist*, 38, 1215–1232.
- RUDOLF, P.R. & GARCES, J.M. (1994): Rietveld refinement of several structural models for mordenite that account for differences in the X-ray powder pattern.– *Zeolites*, 14, 137–146.
- ŞENGÖR, A.M.C. & YILMAZ, Y. (1981): Tethyan evolution of Turkey: A plate tectonic approach.– *Tectonophysics*, 75, 181–241.
- STOCIA, A.D., TARINA, V., RUSSU, R. & GHERGHE, G. (1992): Structural changes in mordenites revealed by two dimensional Fourier synthesis of X-ray powder diffraction patterns.– *Zeolites*, 12, 706–709.
- TERNEK, Z. (1949): Keşan, Korudağ Bölgesinin jeolojisi [*The geology of Keşan–Korudağ region – in Turkish*].– Unpubl. PhD Thesis, İstanbul University, İstanbul, 78 p.
- TURGUT, S., SİYAKO, M. & DİLKİ, A. (1983): Trakya Havzasının jeolojisi ve hidrokarbon olanakları [*The geology of Thrace basin and hydrocarbon resources – in Turkish*].– *Geological Bulletin of Turkey*, 4, 35–46.
- TURGUT, S., TÜRKASLAN, M. & PERİNÇEK, D. (1991): Evolution of the Thrace sedimentary basin and its hydrocarbon prospectivity.– *European Assoc. Petroleum Geoscientists, Spec. Publ.*, 1, 415–437.
- WINCHESTER, J.A. & FLOYD, P.A. (1977): Geochemical discrimination of different magma series and their differentiations products using immobile elements.– *Chemical Geology*, 20, 325–340.
- YILMAZ, Y. & POLAT, A. (1998): Geology and evolution of the Thrace volcanism, Turkey.– *Acta Vulcanologica*, 10, 293–303.
- YILMAZ, Y., TÜYSÜZ, O., YİĞİTBAŞ, E., GENÇ, Ş.C. & ŞENGÖR, A.M.C. (1997): Geology and tectonic evolution of the Pontides.– In: ROBINSON, A.G. (ed.): *Regional and Petroleum Geology of the Black Sea and Surrounding Region*. AAPG Memoir, 68, 183–226.

Manuscript received September 29, 2004.

Revised manuscript accepted November 11, 2005.

